ELSEVIER

Tectonophysics 320 (2000) 123–139

TECTONOPHYSICS

www.elsevier.com/locate/tecto

Deep crustal structure of the area of intersection between the Shackleton Fracture Zone and the West Scotia Ridge (Drake Passage, Antarctica)

Jesús Galindo-Zaldívar [a,*], Antonio Jabaloy [a], Andrés Maldonado [b], José Miguel Martínez-Martínez [a,b], Carlos Sanz de Galdeano [b], Luis Somoza [c], Emma Surinach [d]

[a] *Departamento de Geodinámica, Universidad de Granada, 18071 Granada, Spain*
[b] *Instituto Andaluz Ciencias de la Tierra, CSIC/Universidad de Granada, 18071 Granada, Spain*
[c] *Instituto Tecnológico Geominero de España, Ríos Rosas, 23, 28003 Madrid, Spain*
[d] *Departament de Geodinàmica i Geofísica, Universitat de Barcelona, 08028 Barcelona, Spain*

Received 28 July 1999; accepted for publication 28 January 2000

Abstract

The Shackleton Fracture Zone, which forms the boundary between the Antarctic and Scotia plates in the Drake Passage, is characterized by a present-day left-lateral motion. The West Scotia Ridge, an extinct spreading centre, formed the oceanic crust of the western Scotia Plate and intersects the Shackleton Fracture Zone in a complex deformed area. Multichannel seismic, gravity, magnetic and multibeam swath bathymetry data were acquired during the ANTPAC 97/98 cruise with the Spanish vessel B/O HESPERIDES in the area of intersection of these two tectonic features. The new data reveal its asymmetrical deep crustal structure, which developed as a consequence of the overprinting of extensional and contractional deformation events. The main seismic features of the crust of the Scotia and Antarctic plates are deep dipping braided reflectors, which may be a consequence of an initial stretching deformation related to the Shackleton Fracture Zone. At present, this fracture zone is characterized by thickened oceanic crust, deformed by reverse and transcurrent faults and locally bounded by areas of crustal thinning. The present morphology of the West Scotia Ridge has the characteristics of slow spreading centres, with a central valley bounded by two elongated highs. However, its structure reveals that after spreading ended, there was a NW–SE contractional deformation event, with a thrust of about 40 km of slip that resulted in asymmetrical crustal thickening. Incipient subduction initiates subparallel to the strike of the spreading centre. This tectonic event may be related to an episode of closure of South America and the Antarctic Peninsula, probably of Pliocene age.

We conclude that in oceanic domains, areas with a weak crust (fracture zones and spreading centres) constitute the most sensitive regions for analysing the regional tectonic evolution since deformation events are better recorded there than in normal oceanic crust.

Keywords: Antarctica; deep crustal structure; Shackleton Fracture Zone; West Scotia Ridge

* Corresponding author. Fax: +34-58-248527.
E-mail address: jgalindo@goliat.ugr.es (J. Galindo-Zaldívar)

0040-1951/00/$ - see front matter
PII: S0040-1951(00)00051-2

1. Introduction

The Shackleton Fracture Zone (SFZ) is located in the Drake Passage, between South America and the Antarctic Peninsula. This fracture zone has a related NW–SE-elongated positive relief more than 2000 m high with respect to the neighbouring oceanic plains (BAS, 1985). In addition, several elongated basins are associated with this structure (Aldaya and Maldonado, 1996; Klepeis and Lawver, 1996). The fracture zone intersects the West Scotia (WSR) and Phoenix–Antarctica ridges (PAR), both extinct spreading centres, and developed a ridge-to-ridge transform zone in the central area of the Drake Passage (Fig. 1). However, the geodynamic evolution of the region (Barker et al., 1991; Larter and Barker, 1991), the seismic activity (Pelayo and Wiens, 1989) and the tectonic data (Galindo-Zaldívar et al., 1996) suggest a complex evolution with strike-slip motions along most of the fracture zone since before 29 My to the Recent. At present, the SFZ is a sinistral transpressive fault zone that connects the Chile Trench with the South Shetland Trench and the southern boundary of the Scotia Plate (Cunningham et al., 1995). This fracture forms part of the sinistral fracture

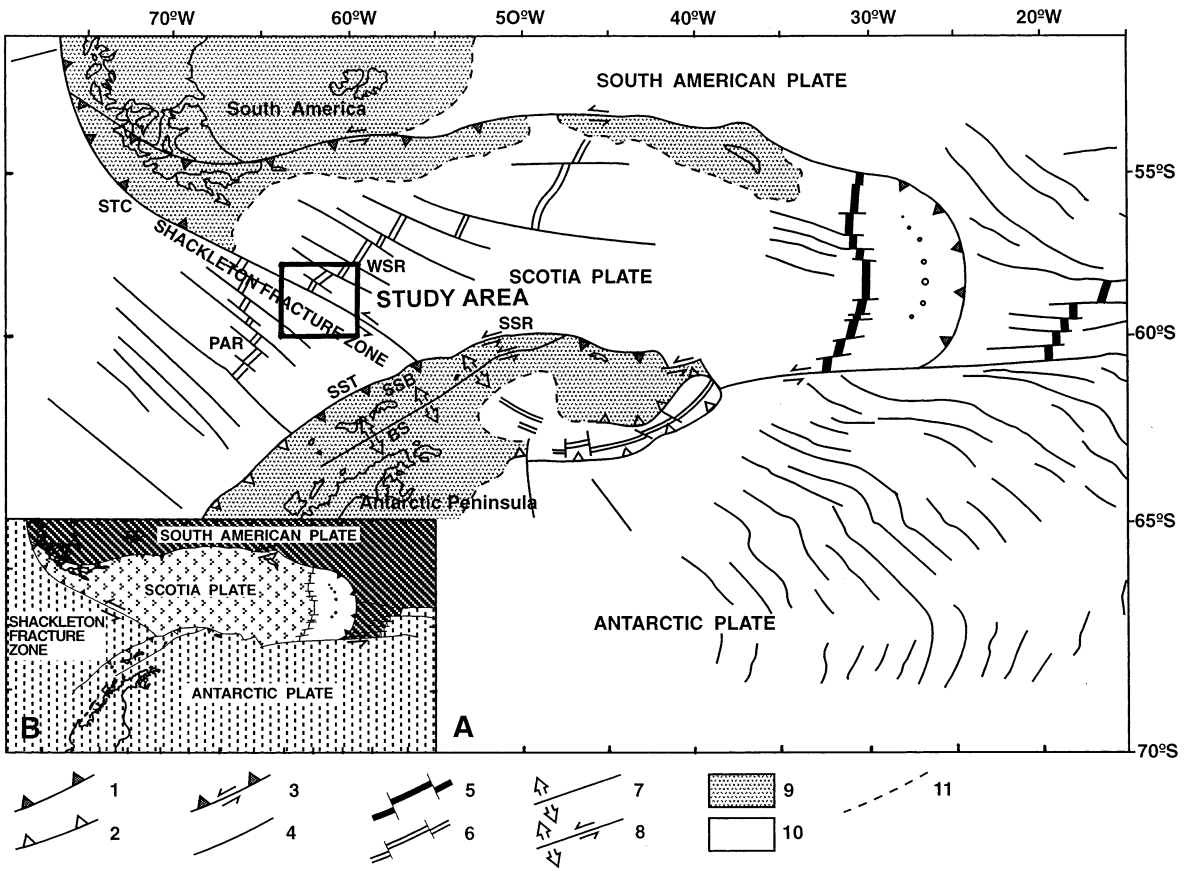

Fig. 1. Geological setting of the study area. 1, active subduction zone. 2, inactive subduction zone. 3, transpressive fault zone. 4, fault zone. 5, active spreading centre. 6, inactive spreading centre. 7, active extensional zone. 8, active transtensional fault zone. 9, continental crust. 10, oceanic crust. 11, continental–oceanic crust boundary. BS, Bransfield Strait; PAR, Phoenix–Antarctic Ridge; SSB, South Shetland Block; SST, South Shetland Trench; STC, South Chile Trench; WSR, West Scotia Ridge. The inset map shows the plate setting.

system that accommodates the relative motion between the South America and Antarctic plates around the Scotia Plate (Livermore et al., 1994).

The crustal thickness remains approximately constant in fracture zones related to fast-spreading centres, whereas intermediate- and slow-spreading centres present associated crustal thinning (Moores and Twiss, 1995). Oceanic transform faults of slow- and intermediate-spreading centres are also generally characterized by elongated deep depressions, individualized from the basin plains by prominent slope scarps (Fox and Gallo, 1984; Moores and Twiss, 1995). Nodal basins are usually located at the intersections of the fracture zones with spreading centres. The triple junctions of fracture zones with intermediate-spreading centres also have related depressions and ridges. However, although the West Scotia and Phoenix–Antarctica ridges show the characteristics of slow- to intermediate-spreading centres, the SFZ has an intricate, prominent relief that seems to record a complex tectonic evolution for these major boundaries (Maldonado et al., in press).

Geochemical and petrological studies of dredged rocks and ophiolites attributed to transform faults indicate that the composition of oceanic crust changes near fracture zones due to the presence of serpentinites (Simonian and Gass, 1978). The diapiric intrusion of serpentinites and upper mantle rocks could develop simultaneously with the evolution of fracture zones (Moores and Vine, 1971; Macdonald et al., 1979; Moores and Twiss, 1995), probably facilitated by an extensional regime.

The morphology, petrology and tectonic evolution of several fracture zones of the world oceans are reasonably well established, but there are fewer studies of the details of the deep structure of these significant regions. The main objective of this contribution focuses on the analysis of the characteristics of the crust of a major fracture zone, the SFZ, which played an important role during the separation of South America and Antarctica. We also aim to contribute to the understanding of the tectonics of the central Drake Passage and the evolution of the plate boundaries in the region, including the West Scotia Ridge spreading centre. With this objective in mind, we mainly analyse multichannel seismic, gravity and swath bathymetry data newly acquired in the area.

2. Data acquisition and processing

During the ANTPAC 97/98 cruise with the Spanish vessel B/O HESPERIDES, multichannel seismic (MCS), swath bathymetry, magnetometry and gravimetry profiles were obtained along several transects in the area of intersection of the SFZ and WSR (Fig. 2). Three MCS and gravimetry profiles were recorded orthogonal to (PRSM06, PRSM08 and PRSM10) and two parallel to the SFZ (PRSM07 and PRSM09), the eastern one cutting across the WSR. Gravity data have been recorded along all of these MCS profiles, and in addition, another five profiles have been measured parallel to the SFZ.

The swath bathymetry was obtained with a SIMRAD EM12 system, processed onboard and visualized with the FLEDERMAUS system at the University of Oregon.

The seismic data were collected with a tuned array of five air guns (total capacity of 22.4 l) and a 2.4 km long, 96-channel streamer. The shot interval was 50 m, and the pressure was 140 atm. The data were recorded with a DFSV digital system with a 2 ms sampling record and 10 s record length. Profiles were processed with a standard sequence, including migration using a DISCO/FOCUS system.

Gravity data were acquired continuously with a Bell Aerospace TEXTRON BGM-3 marine gravimeter. Data were recorded every 10 s after a 3 min filtering interval. The readings were transformed into field values applying the corresponding corrections, using the navigation parameters. Gaps in navigation were corrected by interpolating the data prior to the integration of the navigational parameters with the gravity readings. Profiles were smoothed taking an average of every 300 m. The PRSM10 NE–SW short profile crosses the six long NW–SE profiles and was used for quality control.

In addition, we have taken into account the Geosat free-air gravity data (McAdoo and Marks, 1992) (Fig. 2). There are small differences between

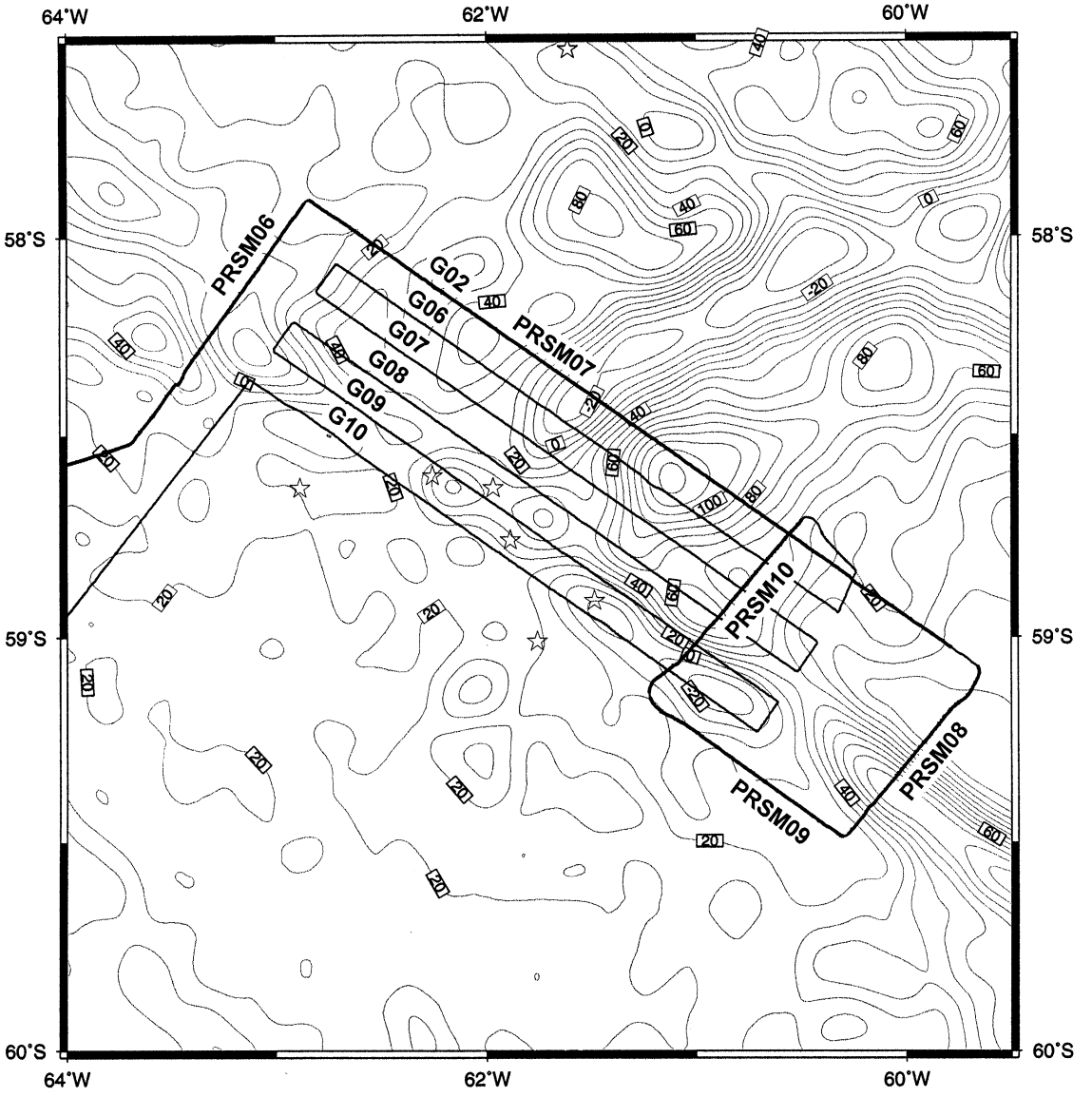

Fig. 2. GEOSAT gravity anomaly map (McAdoo and Marks, 1992) and location chart of the ANTPAC 97/98 cruise with B/O Hesperides track lines. The contour lines are at 10 mgal intervals. Stars: earthquake epicentres (1973–1999), USGS data base. Thick lines, SMC and gravity profiles; thin lines, gravity profiles.

the ship and satellite free-air gravity data in the study region, as shown by the comparison of the profiles cutting across the WSR (Fig. 3). The differences mainly concern the high-frequency anomalies and might be attributed to the different resolution of the two acquisition methods.

3. Seismic structure

The oceanic crusts in the Scotia and Antarctic plates display a very similar seismic stratigraphy, consisting of a discontinuous sediment layer above two igneous layers with different reflectivity pat-

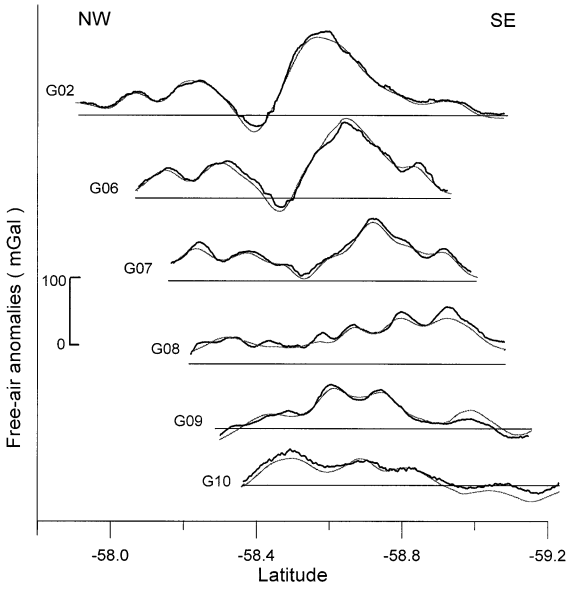

Fig. 3. Comparison of free-air gravity anomaly profiles from the ship survey (thick lines) parallel to the SFZ with those deduced from GEOSAT (thin lines). Profile G02 coincides with profile PRSM07. Other parallel profiles (G) are presented from north to south.

terns (Fig. 4). Very continuous reflectors, mainly confined to small basins, represent the sediment fill. The uppermost layer of the igneous crust shows rough, high-amplitude reflectors at the top and numerous discontinuous high-amplitude reflectors and many irregular diffractions, some of which may be out of plane, in a layer 0.2–0.8 s (TWT) thick. This layer must represent oceanic crust layer 2, primarily composed of extrusives at the top, underlain by sheeted diabase dykes (Francheteau et al., 1992; Mével et al., 1993; Cannat et al., 1995). Below, there is a thicker layer with sparse, weak reflectors that must represent oceanic crust layer 3, considered to be fundamentally formed of isotropic gabbros. The boundary between layers 2 and 3 is progressive and cannot always be located with precision.

The igneous layers locally contain strong, SW-dipping reflectors, in both the Scotia and Phoenix crusts and below the SFZ (Fig. 4A–C). NE-dipping reflectors are also observed, some ascribable to low-angle normal faults (Fig. 4B, profile PRSM10, shot points, SP, 9000–9200). The profiles orthogonal to the SFZ (PRSM06, PRSM08 and PRSM10) show a better development of these dipping reflectors than in the profile PRSM07, orthogonal to the WSR. Dipping reflectors are best observed in the Scotia Plate and show a braided geometry, although neither the top of layer 2 nor the Moho displays large displacements. The sediments are not generally deformed by the structures related to these reflectors. However, in the PRSM10 profile (SP 8900–9100), normal faults with recent activity cut the sediments and continue in depth, defining bands of reflectors. These reflectors reach the base of the crust and dip both to the NE and to the SW.

In some regions, the deepest crustal level is characterized by high-amplitude sub-horizontal, slightly tilted reflectors (Fig. 4). Where these reflectors are more continuous, they may represent the Moho seismic discontinuity (M, Fig. 4). They are distributed between 1.8 and 3.2 s (TWT) below the sea floor, but are preferentially located at a depth of about 2.8–3.0 s (TWT). Locally, short (2–3 km long), very-high-amplitude reflections are observed at a depth of 3.6–4.3 s (TWT) below the sea floor (Fig. 4B). These reflectors are too deep and probably do not represent the crust–mantle boundary. The reflective nature of the upper mantle in the area seems to hamper the precise location of the seismic Moho in some sectors.

The MCS profiles orthogonal to the SFZ show a prominent ridge 2000 m higher than the surrounding ocean floor (Figs. 1 and 4A–C). The relief is symmetrical in profile PRSM08 and asymmetrical in profiles PRSM10 and PRSM06, with the deepest depressions located, respectively, in the SW and NE slopes. The ridge is bounded on both flanks by major faults. On the SW flank, there is a vertical left-lateral strike-slip fault, which has a straight intersection with the bathymetry (Fig. 5; BAS, 1985). The fault on the NE flank of the ridge has a transpressive nature revealed by low-angle, high-amplitude reflectors dipping SW below the ridge (Fig. 4, profile PRSM06, SP50–250; profile PRSM10, SP 8500–8700). The SFZ rocks overthrust the Scotia oceanic crust. The seismic data do not accurately reveal the position of the Moho in this area. The sedimentary cover of the ridge is very scarce or absent. The sediments,

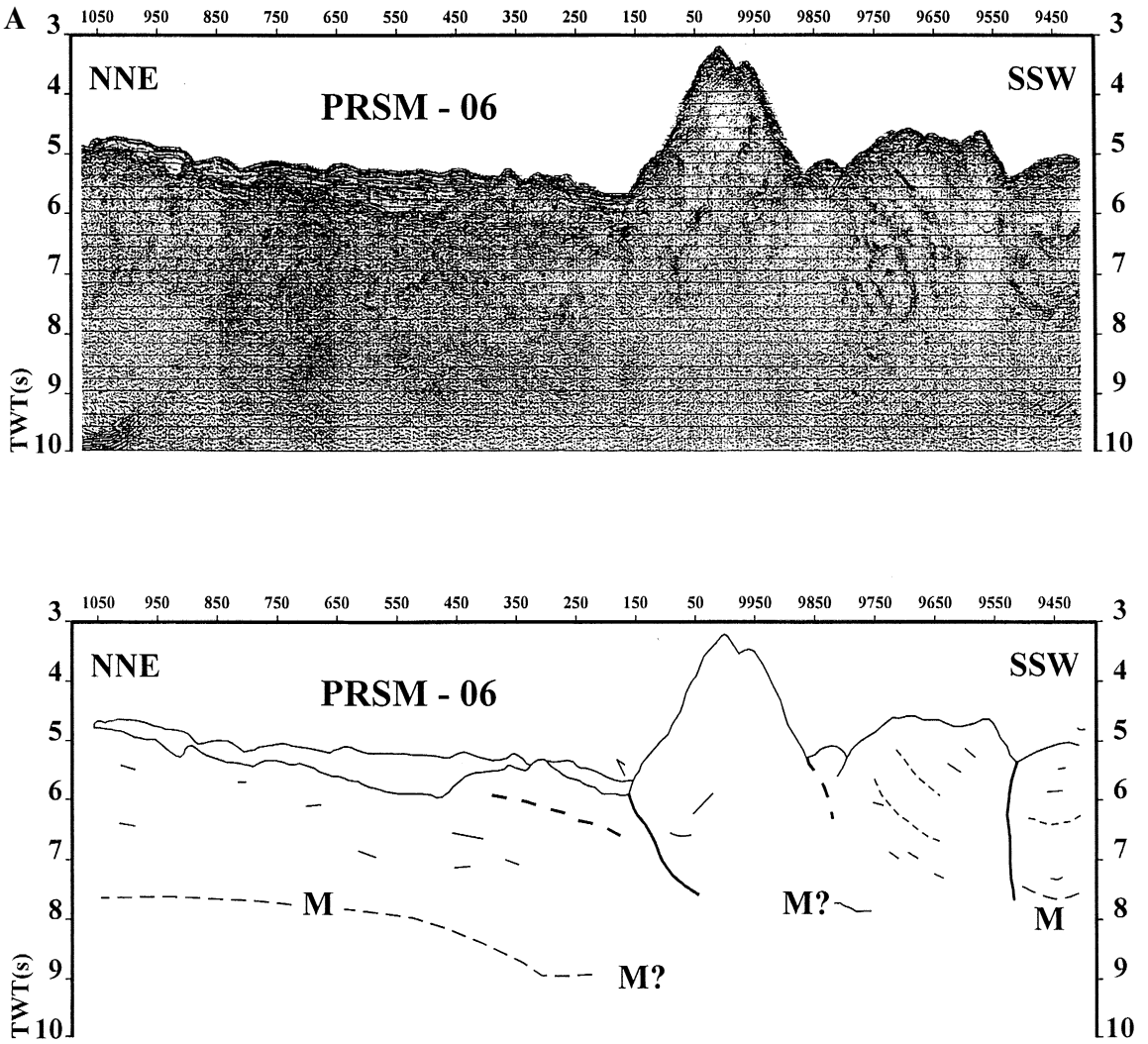

Fig. 4. MCS profiles and interpretation. Location in Fig. 2. M, Moho. 4A, 4B and 4C, profiles across the SFZ. 4D, profile across the WSR.

however, reach a TWT thickness of up to 0.3 s in the oceanic crust near the ridge in profile PRSM08 (Fig. 4C), whereas in profile PRSM06 (Fig. 4A), the sediment thickness varies from 0.8 s near the ridge to 0.2 s at the end of the profile. The sedimentary layer shows basically undisturbed subhorizontal, well-laminated reflectors.

The sea floor of the WSR has an asymmetrical profile (Fig. 4D). The NW flank has a subdued relief, whereas the SE flank is prominent and irregular, becoming smoother and less pronounced away from the spreading centre. The rift valley floor is covered by a depositional sequence 1 s thick (TWT) above the acoustic basement (Fig. 4D). The valley is bounded by high-angle normal faults on both flanks, but the SE fault is more prominent than the NW fault. A SE-dipping reverse fault, affecting the lowermost depositional units and the acoustic basement, is observed along the axis of the central valley in the vicinity of the SE flank. The sedimentary cover is about 0.5 s (TWT) thick in the northern flank of the valley (Fig. 4D, profile PRSM07, SP

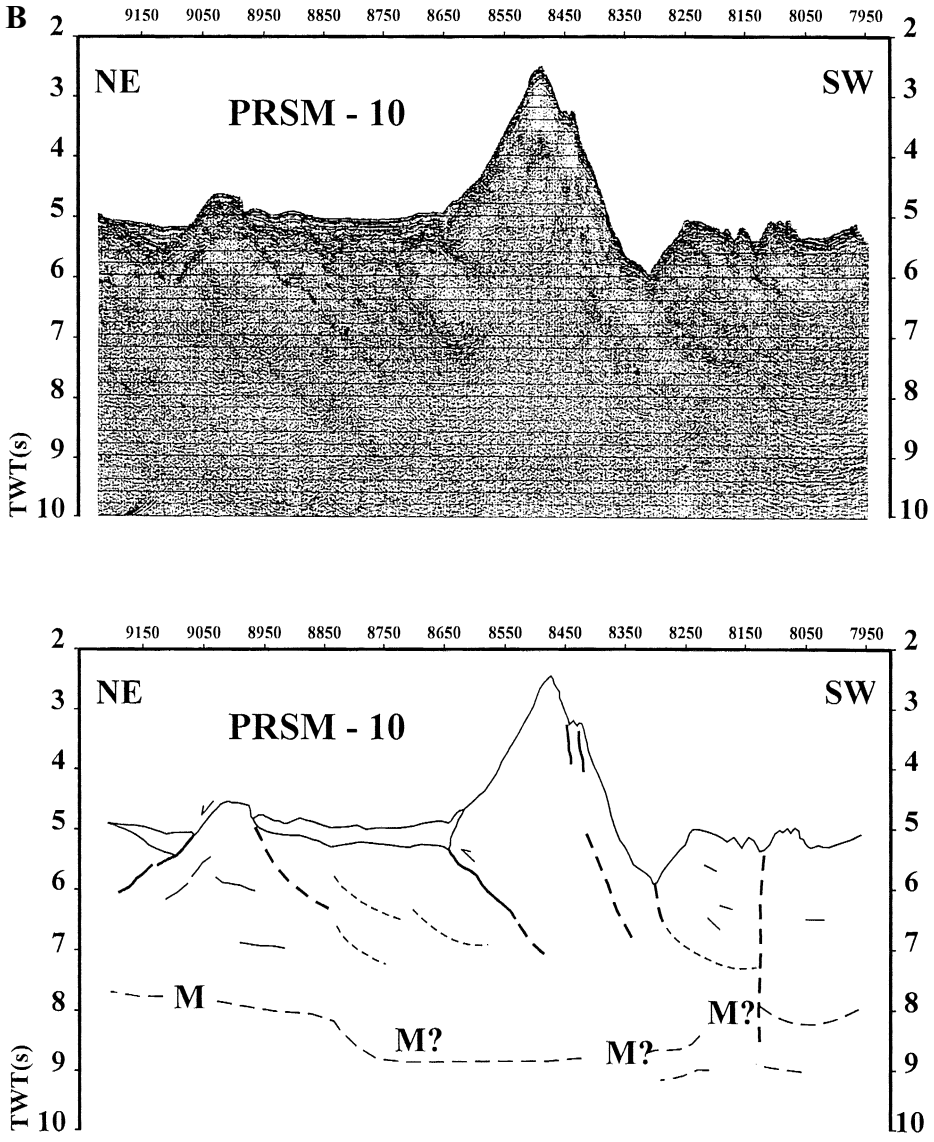

Fig. 4. (*continued*)

2550–2700) and is only observed in a small half-graben on the slope of the southern flank (Fig. 4D, profile PRSM07, SP 3150–3200).

The top of the igneous crust is disrupted by conjugate normal faults. In the flanks, the top of the oceanic crust is generally tilted outward from the central valley, a region in which the basement is tilted southeastwards. As occurs in the SFZ, the seismic data below the extinct spreading centre do not exactly reveal the location of the Moho, although a band of reflectors indicates its position distant from the ridge.

4. Gravimetry

The bathymetry (Figs. 4–6 and BAS, 1985) and free-air anomalies (Figs. 2 and 6) show very good

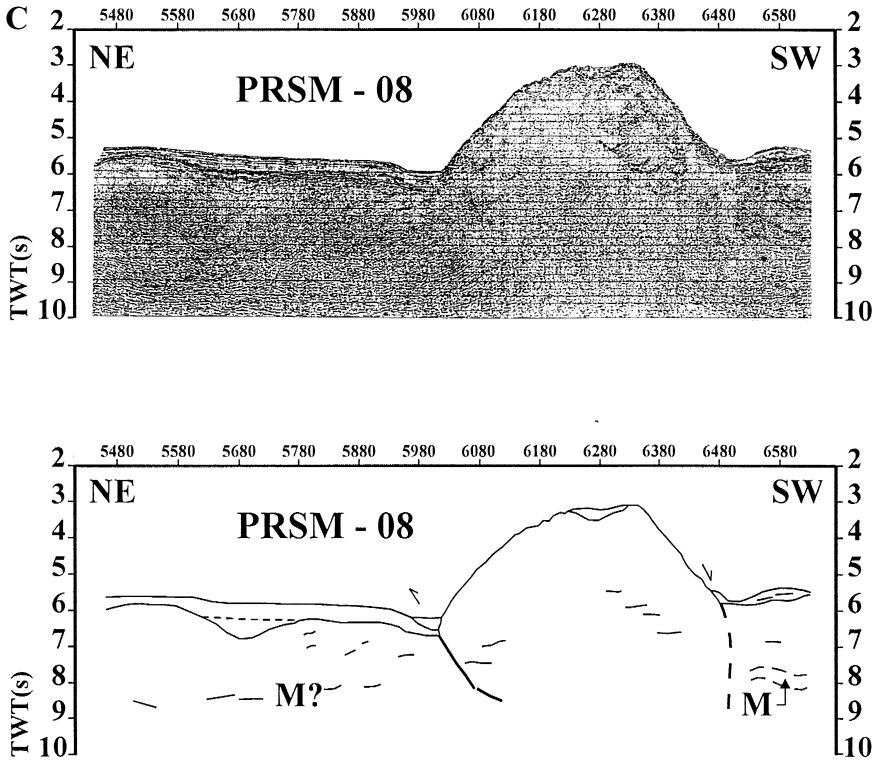

Fig. 4. (*continued*)

agreement in the study area. The SFZ is characterized by a bathymetric and gravity high (2200 m and 90 mGal) bounded by depressions and gravity minima (up to 4400 m and −10 mGal). Free-air anomalies are NW–SE-elongated, parallel to the SFZ trend (Figs. 2 and 5). The free-air gravity profiles cutting across the SFZ are asymmetric, similar to the structures observed in the seismic profiles. In profiles PRSM06 and PRSM08, there is a minimum on the northeastern side, while in profile PRSM10, the most prominent minimum is located on the SW side of the fracture zone (Fig. 6).

The axis of the spreading centre, with a depth of 4100 m, has gravity values down to −20 mGal (Figs. 2, 3 and 6; Profile SM07). Two asymmetric maxima bound the central valley. The SE maximum, with free-air anomalies of up to 125 mGal and 2100 m water depth is higher than the northeastern maximum, where the free-air anomaly reaches values of 50 mGal in areas with a water depth of 3100 m.

Two-dimensional models of free-air anomaly, based on the structure observed in the seismic profiles, have been calculated in order to characterize the location of the Moho below the SFZ and the WSR (Fig. 6). Two-dimensional models are adequate for the analysis of these structures due to the lineal and elongated character of the anomalies observed in the GEOSAT gravity map (Fig. 2). In these models, the geometry of the sea-bottom and the base of the sediment layer were fixed in accordance with the seismic data. We also took into account the location of the Moho in distant regions, where the influence of the SFZ and the WSR structures can be neglected. The typical velocities for the layers identified in the profiles (Fowler, 1990) (1.5 km/s for sea water, 1.8 km/s for sediments, and 5.88 km/s, for the mean of layers 2 and 3 of the oceanic crust) were applied

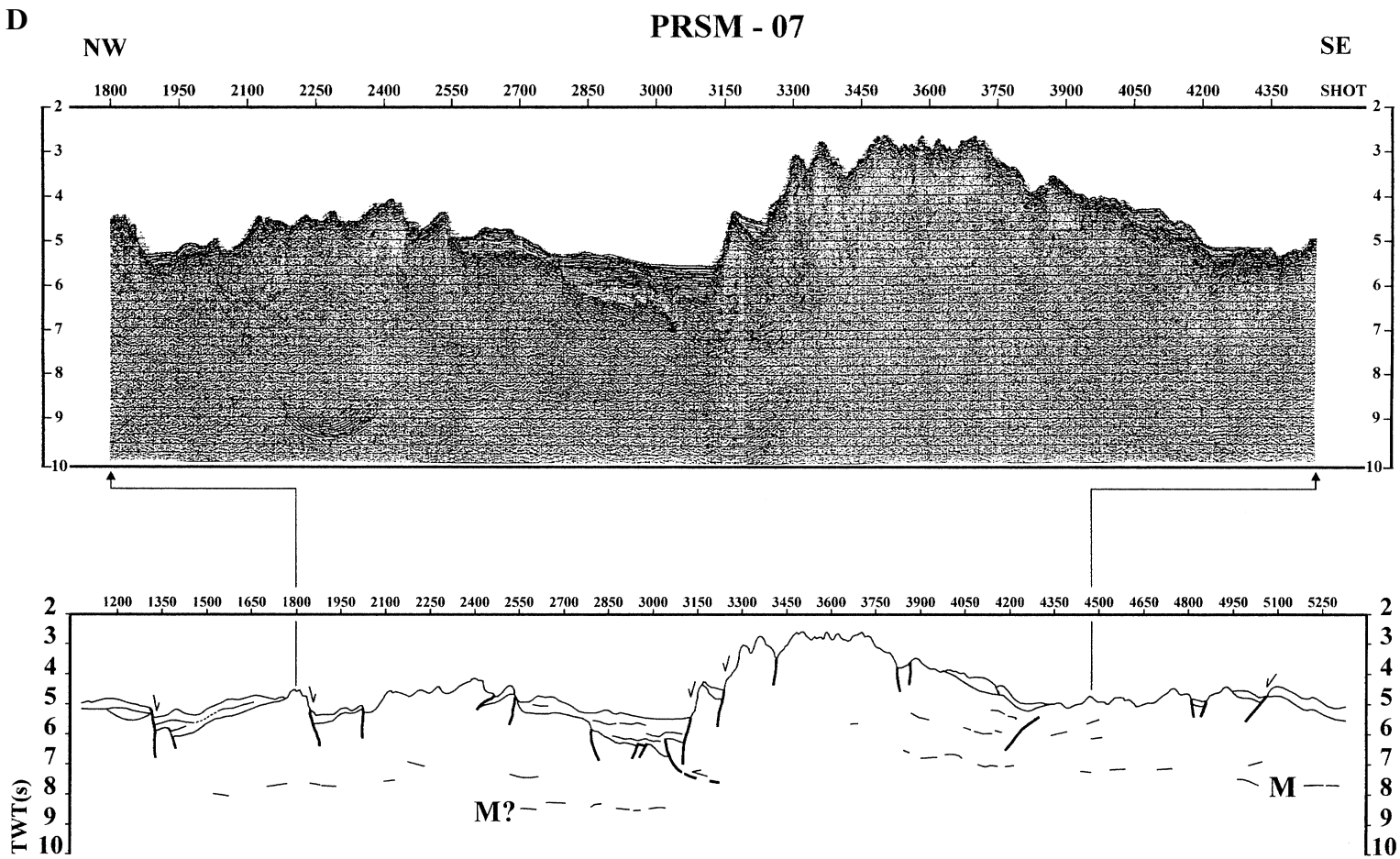

Fig. 4. (*continued*)

Fig. 5. Shaded relief images (Fledermaus) oblique views of the West Scotia Ridge and Shackleton Fracture Zone junction: view towards the south. The length of the area is about 220 km.

for the depth conversion from the time seismic profiles. We have considered the two igneous layers of oceanic crust together since, in most of the profiles, it is difficult to accurately locate their boundary. The following mean densities were also considered for the different layers: sea water, 1.03 g/cm^3; sediments, 2.5 g/cm^3; layers 2 and 3 of the oceanic crust, 2.95 g/cm^3, and mantle, 3.35 g/cm^3 (Fig. 6), taking into account the mean densities of the rocks (Telford et al., 1990) that comprise each layer. However, the models of profiles PRSM06 and PRSM10 display better results by applying a slight decrease in density (2.92 g/cm^3) for layers 2 and 3 in the area of the SFZ. In these profiles, the boundary between the fracture zone body (2.92 g/cm^3) and the surrounding oceanic crust (2.95 g/cm^3) have been placed mainly considering the seismic and bathymetric data, since the contrast in density is not very significant. Furthermore, in the model of profile PRSM08, a slight increase in the density of the igneous crust (from 2.95 to 2.98 g/cm^3) must be applied in order to obtain the best fit of the observed and calculated anomalies, but it is not relevant in the geological interpretation of the model.

The models cutting across the SFZ and the WSR show crustal thickening in these structures (Fig. 6). The crustal thickness varies from 5 to 7 km in normal oceanic crust and up to 11 km in the SFZ and the WSR. The areas bounding the thickened central body of the SFZ also show regions of thin crust, located in the former Phoenix and the Scotia plates (Fig. 6, profiles PRSM06 and PRSM08). The variations in crustal thickness are locally sharp and are related to subvertical faults (profile PRSM06) identified by bathymetry and seismic data and subparallel to the fracture zone (Figs. 4A and 5).

The model cutting across the WSR (Fig. 6,

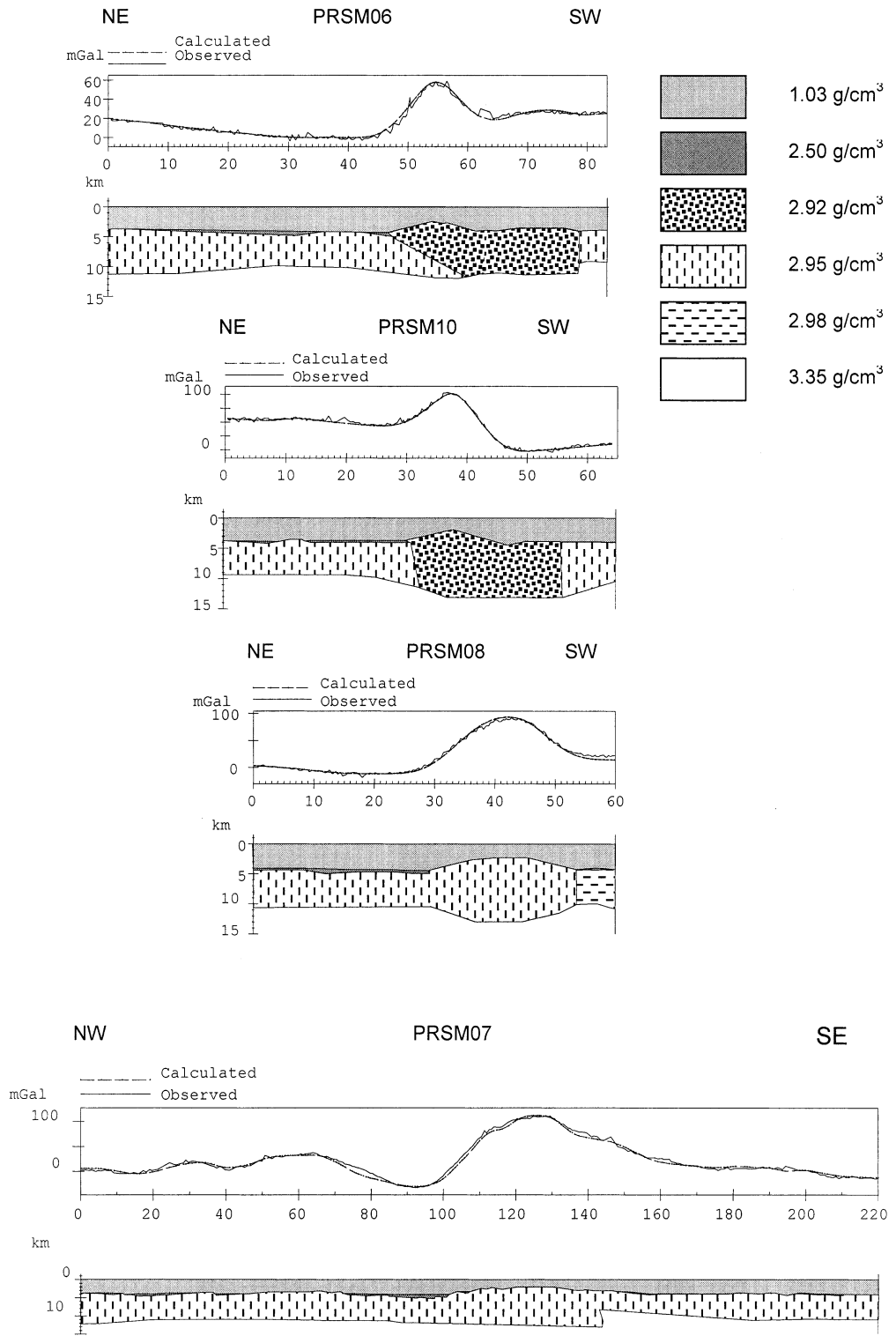

Fig. 6. Free-air gravity profiles and gravity models cutting across the SFZ (PRSM06, PRSM10, PRSM08) and across the West Scotia Ridge (PRSM07) based on MCS profiles. Discussion in the text.

profile PRSM07) shows, similarly to the profiles cutting across the SFZ, that the Moho is asymmetric. The crustal thickness remains almost constant below the central valley, but there is crustal thickening in the southern flank followed by sharp thinning. The differences in crustal thickness displayed by the model indicate large irregularities, from about 5 to 10 km (Fig. 6, profile PRSM07, 130–150 km). The gravity model also suggests a complex geometry, which is justified by the seismic data. The southeastward dipping of the seismic reflectors in the region of the WSR (Fig. 4D, profile PRSM07, SP3650 to 4150) agrees with the proposed shape of the Moho, which regionally dips with the same trend.

5. Discussion

The recently acquired MCS profiles and gravity data allow the structure of the crust in the region of the intersection between the WSR and the SFZ to be established. The deep structure of the crust is derived from the gravity models and complemented by the information from the MCS profiles. The understanding of the tectonic evolution of the area and the proposed models contribute to a better knowledge of the evolution of large oceanic fracture zones and the processes that occur after the extinction of spreading centres.

5.1. Crustal structure

The MCS profiles show the main features of the oceanic crust. Sediments are scarce and irregularly distributed in generally thin, small discontinuous depressions, preferentially on the Scotia plate, controlled by the spreading centre and the fracture zone. The irregular distribution of the sediment cover and its absence west of the SFZ may reflect the influence of the high, irregular relief of the ridge in the circulation patterns of the predominantly eastwards bottom flow across the Drake Passage. The ponded basins of the spreading centre are half-grabens bounded by faults dipping towards the central valley, where the greatest sediment thickness is observed.

The MCS profiles clearly display layer 2 (pillow-lavas), characterized by high-amplitude discontinuous reflectors and a mean thickness of 0.4 s TWT. Since layer 3 (gabbros) is more transparent and its boundary is transitional with layer 2, these two layers have been considered together for the gravity models (Fig. 5). The depth of the Moho, particularly in regions where the MCS profiles do not clearly reveal deep reflectors, as in areas in the proximity of the SFZ and WSR, is estimated in the gravity models constrained by the sectors where the crustal structure is well identified. These models reveal significant crustal thickening under the prominent ridge of the SFZ, which may be elevated at least partially due to the tendency to isostatic equilibrium.

The crust and upper mantle are reflective in the profiles orthogonal to the SFZ and WSR. Although dipping reflectors may originate due to compositional variations in the magma chamber during oceanic-crust spreading, it is not very probable that the observed reflectors originated in this way, since they are not very prominent in profile PRSM07 orthogonal to the spreading centre. However, steeply dipping crustal reflectors are best developed in profiles orthogonal to the fracture zone, particularly in layer 3, suggesting a tectonic origin tied to the evolution of the SFZ. The braided and oblique pattern of these reflectors (Fig. 4A and B) is reminiscent of the geometry of boudins. These structures are typical of ductile shear zones, with flattening and extension. These large-scale, braided bands of oblique reflectors can be interpreted as extensional shear zones that possibly deformed the oceanic crust in early stages of its evolution. This crustal extension could be attributed to transtensional and extensional regimes of the oceanic crust, probably connected to the evolution of the fracture zone. The curvatures of the fracture-zone faults and fault-relay geometry could originate pull-apart basins and local extensional settings. At present, however, there are not enough data to propose a detailed tectonic model to account for these patterns of deformations.

5.2. Structure of the WSR

The WSR is a relict spreading centre revealed by the bathymetry (BAS, 1985) and gravimetry

(Livermore et al., 1994), in which the most recent magnetic anomaly recognized is 5 (BAS, 1985) or 3A (Maldonado et al., in press), and by the existence of a central valley covered by almost undeformed sediments (Fig. 4D). The morphological features of the WSR are characteristic of slowly spreading centres, with a depressed central valley flanked by two prominent, elongated NE–SW ridges. The bathymetric and gravity anomaly profiles are clearly asymmetric, and the SE high is more prominent than the NW high. The gravity model also indicates great asymmetry in the depth of the Moho and does not show, in contrast with active spreading axes, any decrease in depth along the axis of the central valley. The thicker and thinner crusts are located in the regions adjacent to the SE flank. This anomalous distribution of crustal thicknesses suggests that there have been large deformations after oceanic spreading ended. The existence of a thrust in the oceanic crust southeastward of the central valley with a slip of nearly 40 km (Figs. 6 and 7) may justify: (1) the reverse faults that deform the oldest sediments of the central valley; (2) the asymmetry of the Moho depth; (3) the asymmetry of the central valley; (4) the doming of the reflectors in the SE flank (Fig. 4D), which may correspond to a possible accommodation fold; and (5) the obliquity between the bathymetric slope and the anomaly bands of the oceanic crust observed in BAS (1985).

The existence of contractional deformations in the oceanic crust of the Scotia Sea has also been documented in several regions such as the South Scotia Ridge (Aldaya and Maldonado, 1996; Galindo-Zaldívar et al., 1996; Lodolo et al., 1997; Maldonado et al., 1998) and North Scotia Ridge, in the area of the Burdwood Bank (Platt and Philip, 1995). Moreover, in the Antarctic Plate, other compressional structures have been recognized, such as those located in the Bellinghausen region (Gohl et al., 1997). The thrust observed in the WSR probably developed after the end of oceanic spreading and must have been active until the deposition of the bottom unit of the central valley sediments, which are deformed by folds and reverse faults. The thrust is not located in the axis of the spreading centre, but probably developed along weaknesses in the southern flank. The inactive spreading centre is located in the footwall block, and the end of spreading was probably influenced by the contractional event. As a result of this thrusting, some of the magnetic anomalies are obliterated or compressed, making it difficult to precisely establish the end of spreading in the WSR.

The normal faults in this region generally dip towards the central valley of the WSR (Profile PRSM07, Fig. 4D). The relationship of these faults with the scarce sediments indicates that some faults formed contemporaneously with oceanic spreading and the development of the oldest deposits, whereas other faults cut all the depositional

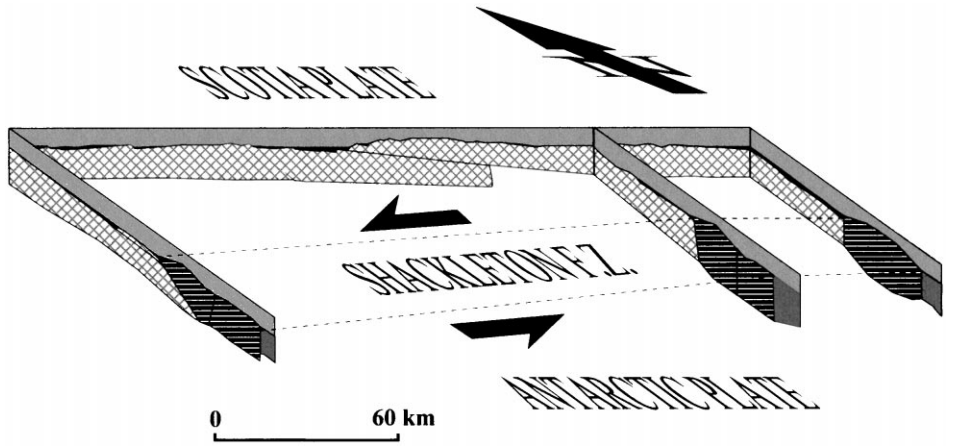

Fig. 7. Perspective sketch of the crustal structure based on gravity models of Fig. 6.

sequences and have undergone recent tectonic activity. As a result of this complex tectonic evolution, the region has experienced alternating extensional and contractional events, which are recorded in the present-day structure of the crust.

5.3. Structure of the SFZ

Seismic, gravity and bathymetric data indicate that the SFZ constitutes a region of crustal thickening. There are also, on both sides of the axial ridge, local depressions and areas of crustal thinning, typical of fractures zones associated with slow-spreading centres. The profiles across the fracture zone are clearly asymmetric and reveal that the structure is similar on both sides of the intersection with the WSR. The main deformation consists of a thrust of the rocks of the fracture zone over the oceanic crust of the Scotia plate, which affects the recent sediments (Figs. 4, 6 and 7). Profile PRSM06 (Fig. 4A, SP 150-450, and Fig. 6) shows a body located on layer 2 of the oceanic crust of the Scotia Sea that may constitute a slice related to this thrust system. The contact of the fracture zone with the extinct Phoenix plate is generally a vertical fault, with a straight bathymetric trace and associated crustal thinning (Figs. 4–7).

In summary, the SFZ represents a structure with transpressive deformation in which the main faults are thrusts with NE vergence responsible for the crustal thickening and subvertical transcurrent faults that bound the fracture zone on its west side. The existence of these structures is compatible with the stress field determined by right-dihedra diagrams of focal mechanisms (Galindo-Zaldívar et al., 1996), which indicate WNW–ESE subhorizontal compression and approximately subvertical extension. The existence of abundant fractures in this sector may have facilitated moderate serpentinization of the mantle rocks and the possible injection through the oceanic crust of serpentinites as occurring in other fracture zones (Moores and Vine, 1971; Simonian and Gass, 1978; Macdonald et al., 1979; Moores and Twiss, 1995). Although this process may be suggested by the slightly lower density of the fracture-zone rocks in the gravity models, the difference in density is not overly significant and may be of only moderate importance in the SFZ.

The proposed structure is clearly different from that suggested by Kim et al. (1997) for the SE end of the SFZ. They propose a marked ascent of the Moho under the fracture zone, which contrasts with the crustal thickening determined in our analysis for the central sector of the SFZ. These differences are probably a consequence of the very low density (2.45 g/cm^3) considered by Kim et al. (1997) for the uppermost unit of the SFZ rocks, which is in the lower range of the serpentinite rocks. Whereas, in our model, serpentinite injection may have some importance, in the model of Kim et al. (1997), most of the upper part of the SFZ is composed of serpentinites. In addition, their model does not consider the subvertical faults related to the SFZ that we found in our study area.

5.4. Constraints for the tectonic evolution model

The results of this analysis allow us to propose a model of the tectonic evolution of the area, considering the present-day crustal structure to be a consequence of the overprinting of contractional and extensional deformation events. Oceanic spreading started in the western Scotia Sea during the late Oligocene (magnetic anomalies 10 or 8), with the rifting of the Antarctic Peninsula and South America (Barker et al., 1991). The region of the Scotia Plate studied, in the central Drake Passage, has an oceanic crust of Miocene to lowermost Pliocene age (anomalies 6 to 3A, Maldonado et al., in press). The magmatic lineaments and magnetic anomalies (BAS, 1985) reveal a NW–SE trend of oceanic spreading. During the opening of the Scotia Sea, normal faults developed dipping towards the spreading centre. Some faults produced asymmetric depressions where the oldest sediments of the region were deposited. When spreading was active at the WSR and the Antarctic–Phoenix ridges, the SFZ constituted a transform fault between these two spreading centres. A transtensional regime or fault relay with the development of pull-apart basins in this young oceanic crust may have induced crustal thinning, in which the deformation was distributed in braided crustal extensional shear zones.

Spreading ended in the WSR when the ridge jumped to the East Scotia Sea and the tectonic regime in the area became inverted, from extensional to compressional. The main contractional structure was the thrust of the oceanic crust of the southeastern Scotia Sea onto the spreading centre. The associated reverse faults affected the lower depositional units of the central valley, which underwent incipient subduction. The thrusting produced a major asymmetry of the structures produced by the old spreading centre, including the central valley and the crustal thickening of the southern flank. A broad hanging-wall anticline also developed, forming the high relief of the southern flank of the ridge. Since the youngest magnetic anomaly recognized in the WSR is 3A (6.6–5 My), the contractional event could be Pliocene or younger.

After the NW–SE contractional episode, there was a new event of normal faulting that formed half-graben structures, generally dipping towards the central valley. Some of these faults seem to affect very recent sediments and are probably old reactivated normal faults. Although some normal faults near the central valley may have been active during thrusting and represent upper plate extension, these structures continue to develop after the end of the thrusting and are also found far from the central valley (Fig. 4D). These faults imply a N–S- to NW–SE-oriented extension of the region. During this event, the SFZ rocks also thrust over the Scotia plate, involving the most recent sediments. There were also active subvertical transcurrent sinistral faults, with associated local crustal thinning. These structures are characteristic of transpressive fault zones and finally produced regional crustal thickening responsible for the present-day bathymetry. Moreover, they are compatible with the current stress field determined by focal mechanisms, with WNW–ESE subhorizontal compression.

Thrust structures in oceanic crust related with old transpressive plate boundaries have also been described in the Bellinghausen Sea (Gohl et al., 1997) and may be a common feature of oceanic crust boundaries. None the less, the main difference between the structure of the Bellinghausen Sea and that of the WSR and the SFZ is the absence of crustal thickening, bathymetric elevation and the more advanced development of subduction in comparison to the WSR and SFZ structures. These differences are probably due to the lower amount of slip and the younger age of the oceanic crust in the study area.

6. Conclusions

The oceanic crust is thickened in the WSR and the SFZ with respect to the normal oceanic crust distant from these structures. The crustal structures of the SFZ and the WSR are the result of the overprinting of compressional and extensional deformation events.

The SFZ is currently active and has similar structures on both sides of its intersection with the WSR, characterized by the thrust of the fracture-zone rocks over the oceanic crust of the Scotia plate. This thrust has contributed to the crustal thickening and to the bathymetric elevation. Moreover, transcurrent sinistral faults have been identified, leading to local crustal thinning.

The braided oblique reflectors identified in the crust in profiles orthogonal to the SFZ could correspond to extensional shear zones, probably forming in relation to transtensional settings associated with the transcurrent faults. Some of these shear zones have recently been reactivated as normal faults that affect the younger depositional sequences. The intense fracturing of this region has most likely contributed to the serpentinization of the upper mantle and possibly to scarce injection of serpentinites into the oceanic crust.

The WSR has a geometry similar to slow-spreading centres, although it shows the overprinting of extensional structures (normal faults dipping towards the central valley), active prior to, possibly during and after the development of a thrust of oceanic crust with an approximate slip of 40 km. The oldest depositional sequences in the central valley are deformed by a reverse fault and represent incipient oceanic subduction produced by the northwestward thrusting of the oceanic crust on the SE side of the WSR.

Spreading ended at the WSR after the late Miocene, likely caused by a change in regional stress field conditions from extension to compression. Contraction along the WSR was apparently simultaneous with the development of contractional structures observed in the southern and northern boundaries of the Scotia Plate. The SFZ and WSR recent deformations are compatible with the present-day WNW–ESE subhorizontal compressive stress field.

Thrust development in oceanic crust during contractional deformation occurred preferentially along zones of crustal weakness, such as fracture zones and spreading centres. In the central Drake Passage, the main expression of the compressional stress field in these young oceanic crusts was crustal thickening, and development of asymmetric bathymetric highs at the SFZ and WSR. The WSR is an interesting case of incipient subduction at a spreading centre. Thus, oceanic plate boundaries seem to be the loci of deformations associated with changing plate kinematics.

Acknowledgements

We acknowledge with gratitude the cooperation of the Commander, officers and crew of the B/O HESPERIDES, who made it possible to obtain these data. We also thank the technicians participating in the cruise for their dedication and help. The diligence and expertise of engineers E. Litcheva and J. Maldonado, who processed the MCS data and swath bathymetry, are appreciated. We are indebted to Dr Ch. Goldfinger, University of Oregon, for facilitating the use of the program FLEDERMAUS to visualize the swath bathymetry and to Dr A. Carbó, for the program Lanzada to calculate gravimetric anomalies. We thank Dr K. Gohl and Dr D. Cunningham for their helpful reviews. We also acknowledge the aid of Christine Laurin in revising the English. The Spanish 'Comisión Interministerial de Ciencia y Tecnología' (CYCIT) provided financial support through Research Project ANT99-0817.

References

Aldaya, F., Maldonado, A., 1996. Tectonics of the triple junction at the southern end of the Shackleton Fracture Zone (Antarctic Peninsula). Geo-Mar. Lett. 16, 279–286.

Barker, P.F., Dalziel, I.W.D., Storey, B.C., 1991. Tectonic development of the Scotia Arc region. In: Tingey, R.J. (Ed.), Antarctic Geology. Oxford University Press, Oxford, pp. 215–248.

BAS, 1985. Tectonic Map of the Scotia Arc Sheet (Misc) 3 Scale 1: 3 000 000. British Antarctic Survey, Cambridge.

Cannat, M., Karson, J.A., Miller, D.J., et al., 1995. In: Proceedings Ocean Drilling Program Leg 153, Init. Rep. College Station, TX (Ocean Drilling Program), pp. 5–13.

Cunningham, W.D., Dalziel, I.W.D., Lee, T.Y., Lawver, L.A., 1995. Southernmost South America–Antarctic Peninsula relative plate motions since 84 Ma: Implications for the tectonic evolution of the Scotia Arc region. J. Geophys. Res. 100, 8257–8266.

Fowler, C.M.R., 1990. The Solid Earth: An Introduction to Global Geophysics. Cambridge University Press, Cambridge, 472 pp.

Fox, P.J., Gallo, D.G., 1984. A tectonic model for ridge–transform–ridge boundaries: implications for the structure of ocean lithosphere. Tectonophysics 104, 205–242.

Francheteau, J., Armijo, R., Cheminée, J.L., Hekinian, R., Lonsdale, P., Blum, N., 1992. Dyke complex of the East Pacific Rise exposed in the walls of Hess Deep and the structure of the upper oceanic crust. Earth Planet. Sci. Lett. 111, 109–121.

Galindo-Zaldívar, J., Jabaloy, A., Maldonado, A., Sanz de Galdeano, C., 1996. Continental fragmentation along the South Scotia Ridge transcurrent plate boundary (NE Antarctic Peninsula). Tectonophysics 242, 275–301.

Gohl, K., Nitsche, F., Miller, H., 1997. Seismic and gravity data reveal Tertiary interplate subduction in the Bellinghausen Sea, southeast Pacific. Geology 25, 371–374.

Kim, Y., Jin, Y.K., Nam, S.H., 1997. Crustal Structure of the Shackleton Fracture Zone in the Southern Drake Passage Antarctica. In: Ricci, C.A. (Ed.), The Antarctic Region: Geological Evolution and Processes. Terra Antarctica Pub., pp. 661–667.

Klepeis, K.A., Lawver, L.A., 1996. Tectonics of the Antarctic–Scotia plate boundary near Elephant and Clarence Islands, West Antarctica. J. Geophys. Res. 101, 20211–20231.

Larter, R.D., Barker, P.F., 1991. Effects of ridge crest–trench interaction on Antarctic–Phoenix spreading: Forces on a young subducting plate. J. Geophys. Res. 96, 19586–19607.

Livermore, R., McAddo, D., Marks, K., 1994. Scotia Sea tectonics from high resolution satellite gravity. Earth Planet. Sci. Lett. 123, 255–268.

Lodolo, E., Coren, F., Schreider, A.A., Ceccone, G., 1997. Geophysical evidence of a relict oceanic crust in the South-western Scotia Sea. Mar. Geophys. Res. 19, 439–450.

Macdonald, K.C., Kastens, K., Miller, S., Spiess, F.N., 1979.

Deep-tow studies of the Tamayo transform fault. Mar. Geophys. Res. 4, 37–70.

McAdoo, D.C., Marks, K.M., 1992. Gravity fields of the Southern Ocean from Geosat data. J. Geophys. Res. 97, 3247–3260.

Maldonado, A., Zitellini, N., Leitchenkov, G., Balanyá, J.C., Coren, F., Galindo-Zaldívar, J., Lodolo, E., Jabaloy, A., Zanolla, C., Rodríguez-Fernández, J., Vinnikovskaya, O., 1998. Small basin development along the Scotia/Antarctica plate boundary and northern Weddell Sea. Tectonophysics 296, 371–402.

Maldonado, A., Balanyá, J.C., Barnolas, A., Galindo-Zaldívar, J., Hernández, J., Jabaloy, A., Livermore, R., Martínez, J.M., Rodríguez-Fernández, J., Sanz de Galdeano, C., Somoza, L., Suriñach, E., Viseras, C. Tectonics of an extinct ridge-transform intersection, Drake Passage (Antarctica). Mar. Geophys. Res. in press.

Mével, C., Gillis, K., Shipboard Scientific Party 1993. Introduction and principal results. In: Gillis, K., Mével, C., Allan, J. et al., (Eds.), 1993 Proceedings Ocean Drilling Program Leg 147 Init. Rep., College Station, TX (Ocean Drilling Program), pp. 5–14.

Moores, E.M., Vine, F.J., 1971. The Troodos massif, Cyprus, and other ophiolites as oceanic crust: evaluation and implications. Philos. Trans. R. Soc. London 278A, 443–466.

Moores, E.M., Twiss, R.J., 1995. Tectonics. W.H. Freeman and Company, New York, 415 pp.

Pelayo, A.M., Wiens, D.A., 1989. Seismotectonics and relative plate motions in the Scotia Sea region. J. Geophys. Res. 94, 7293–7320.

Platt, N.H., Philip, P.R., 1995. Structure of the southern Fakland Islands continental shelf: initial results from new seismic data. Mar. Petrol. Geol. 12, 759–771.

Simonian, K., Gass, I.G., 1978. Arakapas fold belt, Cyprus, a fossil transform fault. Geol. Soc. Am. Bull. 89, 1220–1230.

Telford, W.M., Geldart, L.P., Sheriff, R.E., 1990. Applied Geophysics. Cambridge University Press, Cambridge, 770 pp.